An improved method for feeding ash model compounds to a bubbling fluidized bed – CLC experiments with ilmenite, methane, and

Original Research Article

GREENHOUSE GASES SCIENCE AND TECHNOLOGY

An improved method for feeding ash model compounds to a bubbling fluidized bed – CLC experiments with ilmenite, methane, and K_2CO_3

Felicia Störner, Department of Space, Earth and Environment, Chalmers University of Technology, Göteborg, Sweden
Pavleta Knutsson and Henrik Leion, Chemistry and Chemical Engineering, Chalmers University of Technology, Göteborg, Sweden
Tobias Mattisson and Magnus Rydén, Department of Space, Earth and Environment, Chalmers University of Technology, Göteborg, Sweden

Abstract: Biomass conversion with carbon capture and storage (Bio-Energy CCS; BECCS) is one of the options considered for mitigating climate change. In this paper, the carbon capture technology chemical-looping combustion (CLC) is examined in which the CO_2 is produced in a stream separate from the combustion air. A central research topic for CLC is oxygen carriers; solid metal oxides that provide oxygen for the conversion process. Biomass and waste-derived fuels contain reactive ash compounds, such as potassium, and interactions between the oxygen carrier and the ash species are critical for the lifetime and performance of the oxygen carrier. This work develops and demonstrates an improved method for studying the interactions between ash species and oxygen carriers. The method uses a lab-scale reactor operating under fluidized conditions, simulating CLC batch-wise by switching between feed gas. The novelty of the setup is the integrated system for feeding solid particles of ash model compounds, enabling the simulation of ash species accumulating in the bed. Ilmenite is a benchmark oxygen carrier for solid fuel conversion and was used in this study to evaluate the method using K_2CO_3 as a model ash compound. Experiments were done at 850 and 950°C. Methane conversion in CLC cycles and fluidization was evaluated with gas analysis and pressure drop measurements. Scanning electron microscopy and energy dispersive X-ray spectroscopy (SEM-EDS) and X-ray diffraction (XRD) analysis of bed particles were done after the experiments to establish changes in the morphology and composition of the ilmenite. The method for feeding the ash model compound was concluded to be satisfactory. At 950°C, K accumulated in the particles forming K-titanates and agglomeration was enhanced with K_2CO_3 addition. The agglomeration mechanism was solid-state sintering between the Fe-oxides forming on the particle surfaces. The bed defluidized at

Correspondence to: Felicia Störner, Department of Space, Earth and Environment, Chalmers University of Technology, Göteborg, SE-412 96, Sweden.
Email: felicia.storner@chalmers.se
Received January 16, 2023; revised April 11, 2023; accepted April 14, 2023
Published online at Wiley Online Library (wileyonlinelibrary.com). DOI: 10.1002/ghg.2218

950°C, but no such effect was seen at 850°C. The method is suitable for studying the Fe-Ti-K system with ilmenite and potassium without the influence of other ash species.

Keywords: ash interactions; chemical-looping combustion; oxygen carrier aided combustion; oxygen carriers; potassium interactions

Introduction

Utilizing oxygen carriers for fuel conversion in chemical-looping combustion (CLC) is a promising method to combust fuel and simultaneously separate CO_2 from the flue gases. The CLC process takes place in two interconnected reactors: one fuel reactor and one air reactor. The fuel is added to the fuel reactor and is converted by reacting with a solid oxygen carrier. The reaction is here exemplified with an oxidized metal oxide as oxygen carrier Me_xO_y and a hydrocarbon C_nH_{2m} as fuel:

$$(2n + m)\,Me_xO_y + C_nH_{2m} \rightarrow (2n + m)\,Me_xO_{y-1} + nCO_2 + mH_2O \quad \text{(R1)}$$

R1 is the net reaction, as solid fuels may need to undergo pyrolysis and gasification prior to reacting with the solid. The oxidizing medium is completely free from N_2 and the flue gas from the fuel reactor is pure CO_2 and H_2O. The reactors are typically fluidized beds, where the oxygen carrier constitutes the bed material. In the second step, the oxygen carrier is transferred to the air reactor in which it is oxidized in contact with air, according to (R2).

$$Me_xO_{y-1} + \frac{1}{2}O_2 \rightarrow Me_xO_y \quad \text{(R2)}$$

The solid circulation rate of the oxygen carrier is adapted to transport sufficient oxygen and sensible heat to the fuel reactor. Heat transport may be needed since R1 can be slightly endothermic for certain combinations of fuel and oxygen carrier. The CLC process is illustrated in Fig. 1.

Since biomass captures CO_2 from the air during its growth, using biomass as fuel in CLC (Bio-CLC) combined with carbon storage (Bio-Energy Carbon Capture and Storage; BECCS) could lead to net negative CO_2 emissions and is suggested as a climate change mitigation measure. CLC of solid biomass has been reviewed by Coppola and Scala[1] and Adánez et al.[2]

Oxygen carriers have also been used as bed material in conventional fluidized bed combustion (FBC). The concept is called oxygen carrier aided combustion (OCAC).[3] The role of the oxygen carriers in OCAC is to facilitate the distribution of oxygen in the furnace and increase oxygen availability in locations with a risk of deficiency. Uneven oxygen distribution in combustion facilities is a common problem, especially for biomass- and waste fuels. These fuels are typically inhomogeneous and have high contents of volatiles and moisture. Especially for waste fuels, the heating value can change significantly over time. The large release of volatiles at the fuel-feeding points can cause emissions of unconverted gas species. Consequently, high air-to-fuel ratios are applied to handle these fuels. However, large air flows are in themselves negative for the overall efficiency of the boiler. Further, a high air ratio might not necessarily be an efficient way to handle for example stagnant zones and hot spots in the bed. Apart from creating an oxygen buffer in the bed, the oxygen carrier also enables solid-gas reactions that are less temperature-dependent than flame combustion. Laboratory-scale experiments have shown that methane can be converted in the bottom bed, where the temperature is too low for proper flame combustion.[4]

OCAC has been implemented in several biomass-fired and waste-to-energy (WtE) plants in Sweden. The implementation has been done with an ilmenite-based bed material commercialized by Improbed AB (a subsidiary of the utility company E.ON.). Large-scale OCAC activities were recently reviewed, with a focus on the status in the Nordic countries.[5] The study found that the load of two municipal solid waste-fired boilers could be increased by around 7% when changing from silica sand to ilmenite.[6,7] It also found that a much lower bed material regeneration rate was possible with ilmenite compared to sand.[6] Furthermore, it was concluded that large quantities of potentially suitable oxygen-carrying materials are produced as by-products in metallurgical

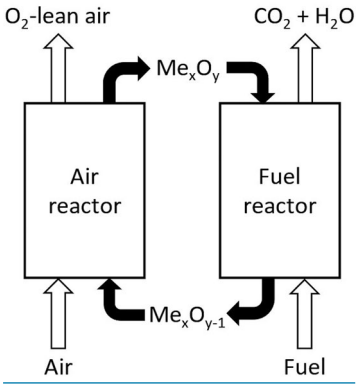

Figure 1. Schematic drawing of the chemical-looping combustion (CLC) process.

industries. OCAC operation is not only a way to improve boiler efficiency but could also accumulate valuable experience in using oxygen carriers on a large scale, and therewith accelerate the development and implementation of CLC.

The current work focuses on the interactions between oxygen carriers and fuel ash and presents an improved method for studying those experimentally. Biomass and waste combustion in fluidized beds require large bed material replacement due to the accumulation of ash in the bed. The same can be expected for CLC and OCAC. A recently published review on CLC of solid biomass concluded that cheap oxygen carriers, like wastes and ores, therefore are the most promising options for biomass CLC.[1] The review further concluded that more research into ash interactions is required for developing industrial-scale use of oxygen carriers.

Biomass ash

The fuel ash composition plays an important role in the combustion process. The ash composition differs widely between different fuels, and some examples are provided in Fig. 2. The figure presents the main ash-forming compounds in bituminous coal, wood, and straw grasses. The data is from the Åbo Akademi Chemical Fractionation Database[8] and the composition is expressed as oxides. The mineral content in coal is typically around 20 wt.-%, but can vary a lot depending on the coal type. When added to the boiler, coal ash mixes with the fluidized bed and is predominantly inert, but can have some oxygen-carrying properties.[9]

Biomass ash differs greatly in composition from coal ash. The mineral content in biomass is typically much lower but the ash that forms is more reactive. The graphs in Fig. 2 show large shares of K_2O and CaO and also quite high fractions of P_2O_5 for biomass fuels. These compounds can take part in chemical interactions with the bed material and the surfaces inside the boiler. Furthermore, other agricultural residues with even more problematic ash compositions might become important fuels in the future.[10] The reactive nature of biomass and waste ash is a big challenge in industrial applications. Accumulation of ash compounds can cause for example corrosion on the superheaters, agglomeration of the bed material, and incomplete combustion.[11,12] Agglomeration can, in turn, cause defluidization of the bed which leads to very costly stops. The negative effects of ash accumulation in the boiler are primarily handled with a replacement of bed material. This is viable in conventional FBC boilers since silica sand is relatively cheap. However, it

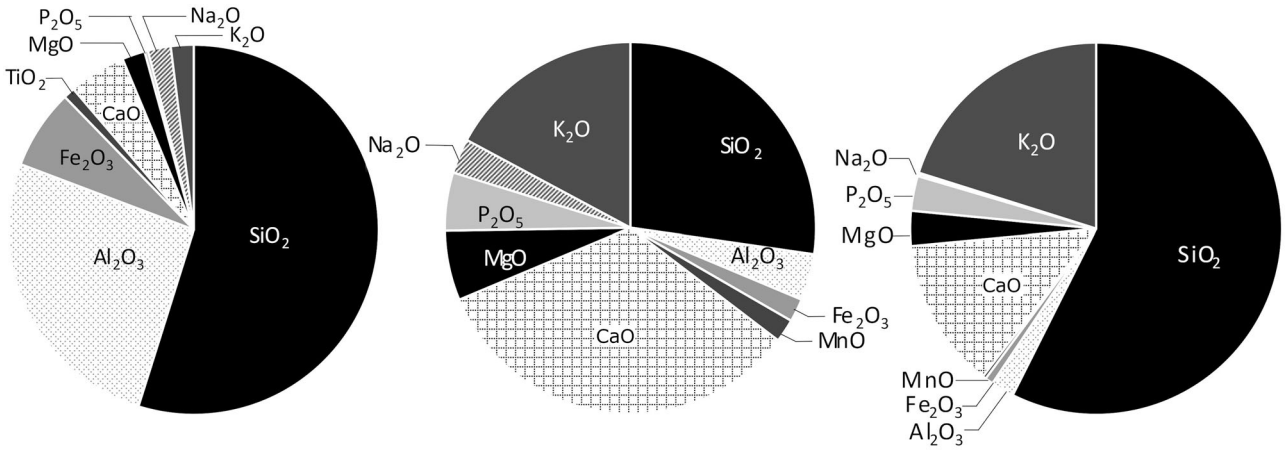

Figure 2. Typical composition of (from left to right) coal ash, wood ash, and straw grasses ash (wt.-%).[8]

might not be feasible when using an oxygen carrier because it might be several times more costly.[5] Thus, it becomes important to know how the lifetime of oxygen carriers is affected by the fuel ash species.

The most problematic ash component is considered to be alkali metals, especially K. Alkali compounds are involved in many unwanted side reactions in the boiler.[13] Gas-phase alkali has also been observed to negatively affect the conversion of CO and contribute to incomplete combustion.[14,15] K exists mainly as soluble salts or as organically bound K ions, some of which can form gaseous compounds. Many attempts have been made to explain the release and reaction paths of K in combustion (e.g.[12,13,16–19,20]). Depending on the form of the alkali and the process conditions, the alkali species will either melt, evaporate, remain as a solid in the bed, end up in the fly ash, etc. In the presence of Cl, K is preferably released as KCl(g), which may deposit on boiler walls which can lead to severe corrosion. In the presence of S, K_2SO_4 is formed, which is less corrosive than KCl. In the absence of Cl and S, K can also exist as K(g) and KOH(g) in reducing and oxidizing conditions, respectively.[13] K_2CO_3 and K_2SO_4 condense and form deposits or fly ash.

In the present study, K_2CO_3 was used as a model compound to simulate the biomass K. K_2CO_3 is a suitable model compound for initial experiments because it is rather stable and has a high melting point. Therefore, it is expected to remain to a large extent in the bed. When inserted in the hot bed, the K_2CO_3 is expected to decompose which releases the carbonate ion as CO_2. K_2CO_3 has been used as a model compound in several fixed-bed interaction experiments (see for e.g., ref. [21–24]).

Ash interactions with bed material

The interaction between ash and bed material in conventional FBC has been examined in several experimental studies.[10,13,25,26] The formation of ash layers on bed particles can be explained to occur via 3 different overall mechanisms[13]: (i) the bed material particle is inert, the ash component deposits on the surface and the layer grows outwards, (ii) the bed material reacts with the ash component and new phases form. The layer grows inwards into the original particle, (iii) the two mechanisms are combined, meaning that some species deposit on the surface and some react with the bed material and diffuse into the particle. The composition and properties of the ash layer thus depend on both the ash and the bed material compositions.

Since oxygen carriers have very different compositions than conventional bed material, mechanism (ii) can be assumed to differ largely from conventional combustion settings. There is also a difference in process conditions since the atmosphere in a CLC fuel reactor is reducing. It is therefore of interest to develop new methods to experimentally investigate interactions between oxygen carriers and different types of ash components.

The oxygen carrier in focus in this study is ilmenite, a mineral that is mined mainly for the production of TiO_2. In oxidized form, the material is pseudobrookite (Fe_2TiO_5). Phase analysis has also shown the presence of $Fe_3Ti_3O_{10}$, Fe_2O_3, and Ti_2O_3.[27,28] The reduced form is ilmenite ($FeTiO_3$) but depending on the composition and degree of reduction, it can also contain magnetite (Fe_3O_4) and even wüstite (FeO) and elemental Fe.[27,21] Reduction from pseudobrookite to ilmenite corresponds to a weight change of about 5 wt.-% of the oxidized material, but a much lower number is expected to be seen in CLC applications. In an experiment by Leion et al.,[29] solid fuel was added during the reduction in such an amount that full conversion corresponded to a 1 wt.-% weight change of the oxidized oxygen carrier. Azis et al.[9] saw an ilmenite reduction by 2 wt.-% during CLC simulation in a batch reactor. A deeper reduction of ilmenite is not likely to occur in CLC or OCAC and could potentially cause sintering of the particles. Purnomo et al. saw sintering in an ilmenite bed when reduced by 3.2 wt.-%.[27]

The changes in ilmenite particles during operation in industrial OCAC settings were studied by Corcoran et al.[30,31] Clear differences were observed between fresh ilmenite and ilmenite that had been in the boiler for a few days. In fresh ilmenite, the iron was evenly distributed across the whole particle, but during OCAC operation, the iron migrated out toward the surface of the particle. This caused the reactivity of ilmenite to increase over time.[32] The reactivity (measured as fuel conversion) is, in fact, quite low for fresh ilmenite.[33] During operation in the boiler, the particle surface became more and more covered in ash components (mainly Ca, Mg, and K-species).[30] It was found that the ash components mainly interacting with the ilmenite were compounds rich in K and Ca.[30] Ca accumulated in the form of $Ca(Ti_{0.7}Fe_{0.3})O_{2.5}$ located in two layers around the particles. K diffused into the particles, forming KTi_8O_{16}. The stability of KTi_8O_{16} has been

Table 1. Previous experimental studies of interactions between ilmenite and ash model compounds.

Study	Model compound	Experiment	Atmosphere	Temp.
Zevenhoven et al.[22]	K_2CO_3	Fluidized bed, continuous feeding	Dry, air	850°C
	K_2SO_4			950°C
	KCl	Fixed bed, mixtures	Dry, air	850°C
	KH_2PO_4			
Hildor et al.[21]	K_2CO_3	Fixed bed, mixtures	Wet, reducing	850°C
	K_2SO_4		Dry, reducing	
	KCl			
	KH_2PO_4	TGA	Wet, cycles	850°C
			Dry, cycles	
Staničić et al.[23]	$CaCO_3$	Fixed bed, mixtures	Dry, air	900°C
	K_2CO_3		Wet, reducing	
	SiO_2			

verified by Staničić et al. with thermodynamic modeling,[34] with the highest stability at low K and reducing conditions, which could potentially be found inside particles. Thus, ilmenite seemed to stabilize the K released from the fuel and hinder it from further interacting with the boiler surfaces. A series of corrosion tests with K-doped ilmenite has led to this conclusion.[35] Further, Gogolev et al.[36] showed with alkali emission measurements in CLC pilot experiments that fuel alkali is largely retained in the ilmenite. They also observed that gas-phase alkali was released mainly in the fuel reactor. These are positive results considering that the superheaters (that are the most critical boiler equipment when it comes to corrosion) are located downstream of the air reactor in CLC. Agglomeration of ilmenite has not been observed in OCAC operation and thus a lower amount of bed material makeup was required during operation compared to when silica sand was utilized as bed material.[5]

Most previous lab-scale experiments examining interactions between oxygen carriers and biomass ash or ash model compounds have been performed using fixed beds (e.g.,[23,21,37,38]). Table 1 shows a summary of experiments with ilmenite and ash model compounds. Only a few studies have utilized fluidized bed reactors (e.g., Zevenhoven et al.,[22] with biomass, and Azies et al.,[9] with coal ash interactions). Fluidized bed interaction experiments are important to simulate a CLC or OCAC process and be able to determine the effect of ash on reactivity and oxygen transfer. Further, solid-solid experiments can provide a valuable view of possible chemical phenomena, but may not provide a proper explanation of what happens in a real system, where the ash components or precursors will not necessarily be in the solid phase when meeting fluidized oxygen carrier particles. Also, in such experiments, it is difficult to directly measure the effect on the oxygen transfer process and the reactivity with the fuel, which are important aspects in real systems. When it comes to ilmenite, understanding the K-Fe-Ti system in the boiler is important for several reasons. K interactions can affect the deposition on the boiler walls, the activity of the oxygen carrier, the possibility of regenerating the bed material, etc.

Aim of the study

The present study has two aims. The first is to develop a method for conducting experiments with interactions between ash model compounds and oxygen carriers under fluidized conditions simulating CLC. The second goal is to study the performance of ilmenite during CLC cycles with a continuously increasing load of the ash model compound K_2CO_3. The performance of the ilmenite is evaluated concerning fluidization and reactivity in redox reactions. This is of high importance as previous studies mentioned above clearly show that K can react and diffuse into the ilmenite lattice. How the reactivity is affected is of high technical importance.

Table 2. Summary of requirements for the new reactor and related design choices.

Requirements	Design
Temperature and corrosion resistance No/little uptake of alkali by the reactor wall: Alkali should be available for reacting with the bed material. Safe to use gaseous fuels at a slight overpressure.	High-temperature steel (253MA). Corrosion resistant Does not absorb alkali Can work with slight overpressure
Feeding of solid alkali salts without melting or clogging inside the feeding system. Contact between salt and bed material is ensured	Connection for sweeping gas. Management of heating zones. Adjustable feeding pipe – trial and error method to find a suitable feed point slightly above or inside the bed.
No cross-contamination of samples.	All parts can be disassembled and cleaned/replaced

Reactor system

Reactor design

For this study, a new lab-scale fluidized-bed reactor has been designed. The requirements and some design implications of those are summarized in Table 2.

A schematic drawing of the reactor is presented in Fig. 3. High-temperature 253MA steel was chosen for the reactor to withstand alkali interactions and corrosion at high temperatures (as has been observed by Mei et al.[39]). Interactions between alkali and reactor walls in experimental systems have been thoroughly examined by Andersson et al.[40] The reactor is made of two pipes connected via flanges welded to the pipes. The inner- and outer diameters of the pipes are 26 and 33 mm. The bottom pipe makes up the wind box. It is 530 mm long and is placed in the furnace so that 380 mm of it is within the heating zone. The top pipe holds the bed and the freeboard. It is 270 mm long, out of which 120 mm is located in the heating zone. Between the two pipes is situated a distribution plate and copper gaskets. The gas distribution plate is a thin, perforated stainless steel plate that generates the pressure drop required for fluidization. Some practical advantages of the steel reactor compared to a quartz reactor are that it is difficult to break and connecting the gas lines is done by screwing them on with metal connections. The design makes it possible to open the reactor at the flanges for cleaning and to replace the distribution plate when required. The purpose of the relatively short freeboard is to have as short a heating time as possible for the salts falling into the bed from the top and facilitate contact between the bed particles

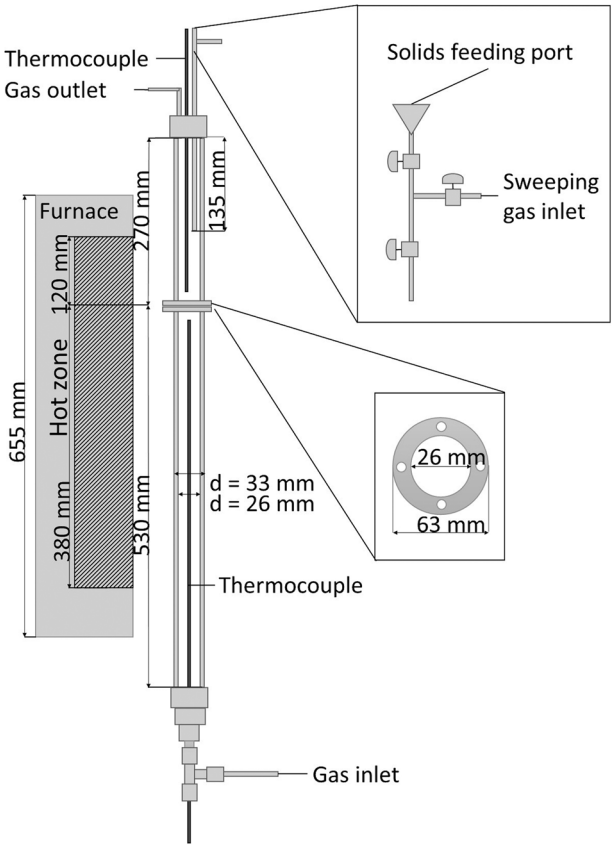

Figure 3. Schematic representation of the new steel reactor. The location of the reactor in the furnace is also indicated.

and the salt. Two thermocouples are located vertically inside the reactor; one from the bottom under the distribution plate and one from the top reaching into the bed. The temperature below the bed is used to

regulate the furnace. The pressure drop over the reactor is continuously monitored. The pressure sensors are located on the ingoing gas line (under the reactor) and the outgoing line (above the reactor). The pressure drop over the fluidized bed is recorded at 10 Hz. A combination of a significant decrease in pressure drop and pressure fluctuations indicates that defluidization and/or agglomeration has taken place. In this case, the bed is still or only partly fluidized and the gas passes through channels in the bed.[22]

Salt feeding system

The salt feeding system is designed to feed salt particles from the top of the reactor through a stainless-steel pipe inserted into the reactor. The pipe has an inner diameter of 6 mm. It is fitted with several ball valves at the top, creating an airlock for the safe addition of salt and a connection for sweeping gas (nitrogen). For the current experiments, a pipe reaching 135 mm into the reactor from the top was used, which is half the freeboard length. The pipe is easily removed and cleaned, replaced, or adjusted to fit the conditions of the experiment.

Experimental setup

The fluidizing gas enters the bottom of the wind box. The feeding of gas into the system is controlled by mass flow controllers. Magnetic valves are used to quickly switch between different gas mixtures, that is, between oxidizing, reducing, or inert flow. The gas outlet is located at the top of the reactor. A sintered metal filter is located after the reactor to capture dust. The gas lines downstream of the reactor are heated to 200°C to avoid condensation of water. Subsequently, the heated gas enters a cooler where the steam is condensed, and the gas is cooled to around room temperature. The resulting dry gas enters a gas analyzer that measures the flow rate and the concentrations of CO_2, CO, CH_4, O_2, and H_2. The gas analyzer is a Rosemount, model NGA-2000. The surrounding experimental infrastructure is explained more in detail by Leion et al.[41]

Experimental procedure

The experiments aimed to simulate a CLC process with a K-rich fuel, during potentially accelerated process conditions. The simulation of fuel ash addition was done by adding low amounts of an ash model compound in regular intervals during batch CLC operation. Details about the procedure for ash addition are presented below. The effect of the accumulation of the ash specie was evaluated during the experiment with respect to gas conversion and pressure drop.

Table 3. Composition of ilmenite on oxygen-free basis (provided by Titania A/S).

Fe	Ti	Si	Al	Mn	Ca	K	Mg
36.46	26.89	0.93	0.34	0.19	0.23	0.02	2.16

Oxygen carrier and chemicals

Ilmenite concentrate was used as an oxygen carrier in the experiments. The ilmenite used has been described by Leion et al.[42] and the composition (on an oxygen-free basis) is presented in Table 3. Before the experiments, the ilmenite particles were heat-treated in air at 950°C for 12 h and sieved to obtain a size fraction of 125–180 μm. 20 g of ilmenite was used as bed material in the experiments. To simulate the accumulation of alkali ash in the bed, K_2CO_3 was used as a model compound. Lehman et al.[43] studied the stability of K_2CO_3 close to its melting temperature under varying CO_2 concentrations. They concluded that the partial pressure of CO_2 had a strong influence on the decomposition of the salt, but that some decomposition took place also at high CO_2 concentrations. The melting temperature of K_2CO_3 was concluded to be around 900°C and to depend on the CO_2-pressure.[43] Thermogravimetric analysis of mixtures of oxygen carriers and K_2CO_3 has shown the decomposition of the salt during heating in an inert atmosphere at around 700–800°C.[21,22,24] When added to the reactor in an inert atmosphere, K_2CO_3 was therefore expected to decompose to K_2O and CO_2, and the vapor pressure of K was expected to be low. During the reducing period, steam forms from the conversion of methane and KOH, which has a higher vapor pressure, could form.[44] The contact of K with the oxygen carrier was assumed to be a combination of solid-, liquid-, and gas-solid in varying fractions depending on the temperature and gas composition.

Activation

The reactivity of fresh ilmenite with gaseous fuels is relatively low but increases in the first few oxidation- and reduction cycles, a process referred to as activation. Activation of ilmenite has been studied by

Table 4. Activation procedure with diluted syngas for reduction and diluted air for oxidation.

Period	Gas flow (NmL/min)	Gas composition	Time
Heating	1000 NmL/min	Air in N_2 (12.4% O_2)	
Inert	1000 NmL /min	N_2	180 s (approx.)
Start of activation cycles			
Reduction	500 NmL/min 500 NmL/min	Syngas N_2	40 s
Inert	1000 NmL /min	N_2	60 s (approx.)
Oxidation	1000 NmL/min	Air in N_2 (12.4% O_2)	Until $CO_{2,\,out} = CO_{2,\,in}$
Inert	1000 NmL /min	N_2	180 s (approx.)

Table 5. Experimental procedure with diluted methane for reduction and diluted air for oxidation.

Period	Gas flow (NmL/min)	Gas composition	Time
Heating	1000 NmL/min	Air in N_2 (12.4% O_2)	
Inert	1000 NmL /min	N_2	180 s (approx.)
Start of experimental cycles with fuel and salt			
Reduction	400 NmLmin	CH_4	40 s
	500 NmL/min	N_2	
Inert	1000 NmL /min	N_2	60 s (approx.)
Oxidation	1000 NmL/min	Air in N_2 (12.4% O_2)	Until $CO_{2,\,out} = CO_{2,\,in}$
Inert[a]	1000 NmL /min	N_2	180 s (approx.)

[a] K_2CO_3 was added to the bed during this inert period preceding the reduction

Adánez et al.[33] and Azis et al.,[9] among others. In the present study, the material was activated before the experiment in this study. Syngas (50% CO and 50% H_2) diluted to 50% with nitrogen was used as reducing gas during the activation. The oxidation was done with diluted air (62% synthetic air in N_2). The conditions in the activation cycles are presented in Table 4.

The heating was done under oxidizing conditions. The bed material activation was then done with a gradually increasing temperature. The reactor was first heated up to 700°C. The first two cycles were performed at 700°C. The temperature was increased to 800°C and several cycles were then performed at 800, 850, 900, and 950°C. In total, around 28 activation cycles were performed with each batch of ilmenite.

Experiments with salt addition

After the activation, the experiments were performed according to Table 5. Experiments without and with the addition of K_2CO_3 were performed at 850°C and repeated at 950°C.

Reducing gas and reduction time

Methane was used as fuel because methane conversion is a good indicator of the reactivity of the oxygen carrier. Complete oxidation of methane takes place according to reaction R3, with a general oxygen carrier Me_xO_y as an oxidizing agent:

$$CH_4 + Me_xO_y \rightarrow CO_2 + 2H_2O + Me_xO_{y-4} \quad (R3)$$

Partial oxidation of methane also results in some H_2 and CO. When the conversion is with an oxygen carrier, there is no gaseous oxygen, and the fuel/product gas volume ratio is 1:3 at complete conversion. The water was condensed after the reactor. Thus, the flow rate to the analyzer was similar in size to that of the reactant gas. Methane has low reactivity with ilmenite and full conversion was not expected, which facilitates the evaluation of how the reactivity develops in contact with ash compounds. When evaluating the results, both methane conversion and degree of oxidation were of interest since methane can be either converted completely to CO_2 or partially

Table 6. Details of the additions of K_2CO_3 during the experiments.

Cycle no.	Addition (mg)	Accumulated (mg)	Wt.-% salt added to the bed	Wt.-% K added to the bed
6	100	100	0.5	0.3
8	100	200	1.0	0.6
10	300	500	2.4	1.4
12	400	900	4.3	2.4
14	400	1,300	6.1	3.5
16	500	1,800	8.3	4.7
18	500	2,300	10.3	5.8

oxidized to CO. Before being fed to the reactor, the methane was diluted with N_2 and the resulting flow was 400 NmL/min CH_4 and 500 NmL/min N_2. The duration of the reducing period was 40 s. Complete conversion of all the ingoing methane would correspond to a weight change of the oxygen carrier by about 3.6% (mass-based conversion, $\omega = 0.964$, defined according to Eqn (1)).

Addition of ash model compound

The gradual accumulation of K-species in the reactor was realized by stepwise addition of low amounts of K_2CO_3. Batches of salt were added during the inert phase after oxidation. Salt addition was immediately followed by reduction, relating to the introduction of ash in the fuel reactor. Five redox cycles were first performed without salt addition to establish a stable starting point. Salt was then added every second cycle, with one cycle in between for stabilization and evaluation of the impact on fuel conversion. The in-between cycles were applied since the addition of K_2CO_3 released CO_2, which complicated the data evaluation. By focusing the reactivity evaluation on the in-between cycles, conclusions could be made about fuel conversion as a function of ash load. In total seven additions were done, in accordance with the scheme shown in Table 6. The salt was added from the top of the reactor (as illustrated in Figure 3) and N_2 was pulsed through the feeding system for 3–4 pulses to facilitate the transport from the feeding port to the bed.

The experiment was concluded after the last reducing phase. The gas was then switched to nitrogen and the furnace was turned off. The reactor was allowed to cool down overnight with a small throughflow of nitrogen.

Data evaluation

Fluidization

The fluidization of the bed was studied qualitatively by continuous measurements of the pressure drop over the bed. A sudden decrease in pressure drop and/or a drastic decrease in pressure drop fluctuation indicated a negative effect on the fluidization of the bed.[22,26,27] The samples were also examined visually to create an understanding of the connection between lump formation and pressure-drop behavior.

Fuel conversion

The gas concentrations from the experiments were used to evaluate the fuel conversion. The parameters used to quantify the fuel conversion performance were the mass-based conversion of the oxygen carrier and the yield of CO_2, CO, and CH_4. The mass-based conversion, ω is defined according to Eqn (1) where m is the instantaneous oxygen carrier mass and m_{ox} is the mass of the oxygen carrier when it is oxidized. Equation (2) was used to calculate ω when methane was used as fuel, ($\dot{n}$ is the molar flow, M_o is the molar mass of oxygen, x is the concentration). The integration was done over the whole reducing period, in this case, 40 s, to obtain the value ω_{flnal}.

$$\omega = \left(\frac{m}{m_{ox}}\right) \times 100 \ [\%] \quad (1)$$

$$\omega = \omega_i - \left(\int_{t_0}^{t_1} \frac{\dot{n} M_o}{m_{ox}} \left(4x_{CO_2} + 3x_{CO} - x_{H_2}\right) dt\right) \times 100 \ [\%] \quad (2)$$

The initial value ω_i was 100 since it is assumed that the oxygen carrier was completely oxidized at the beginning of the reduction and thus $m_i = m_{ox}$. For simplifying the presentation, the value $(100 - \omega_{flnal})$

will be presented since it is proportional to the total fuel conversion.

The CO_2 yield was calculated with Eqn (3), where n_{CO_2} is the number of moles of CO_2 formed. The molar flow of each component was calculated from volume flow and concentrations and integrated over the whole reduction period (Eqn (4)). The yields of CO and CH_4 were calculated in the same way (Eqns 5 and 6). In practice, CH_4 yield means unconverted methane.

$$\gamma_{CO_2} = \frac{n_{CO_2}}{n_{CO_2} + n_{CO} + n_{CH_4}} \quad (3)$$

$$n_{CO_2} = \int_{t_0}^{t_1} \dot{n} x_{CO_2} \mathrm{d}t \quad (4)$$

$$\gamma_{CO} = \frac{n_{CO}}{n_{CO_2} + n_{CO} + n_{CH_4}} \quad (5)$$

$$\gamma_{CH_4} = \frac{n_{CH_4}}{n_{CO_2} + n_{CO} + n_{CH_4}} \quad (6)$$

Material analysis

After the reactor experiments, the bed material samples were collected and subject to material analysis using scanning electron microscopy (SEM) and energy dispersive X-ray spectroscopy (EDS). SEM-EDS analysis was used to obtain information on how exposure to K_2CO_3 changed the composition and morphology of the particles. Samples were prepared in two different ways to study both the surface as well, and the cross-section of sample particles. For surface analysis, particles were mounted on a carbon-taped stub. The samples for cross-section analysis were prepared by mounting particles in epoxy resin and grinding them to obtain a cut cross-section area. The samples were also analyzed by X-ray diffraction (XRD) with a Bruker D8 Discover, to determine the crystalline phases. A copper X-ray source was used, and the analysis was done with a step size of 0.02° in the range of $2\theta = 20 - 90°$.

Results and discussion

The effect of the salt addition to the experiments was evaluated through the pressure drop, conversion of CH_4, and material analysis of extracted bed material. Figure 4 exemplifies one experimental redox cycle. The figure shows the concentrations of CH_4, CO_2, CO, H_2, and O_2 obtained in the 11th cycle of the 850°C experiment without salt addition. $T = 0$ s was when the

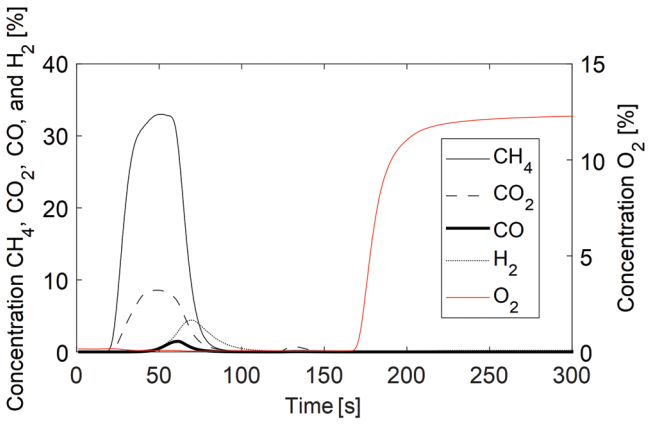

Figure 4. Concentration profile for the 11th cycle in the 850°C experiment without salt addition. The reducing gas flow was on from $t = 0$ to $t = 40$ s. The oxidizing gas flow started at $t = 100$ s.

flow was switched from inert to reducing conditions. There was a delay of approximately 15 s due to the distance between the reactor and the gas analyzer. The oxidizing gas flow started at $t = 100$ s and at the beginning of the oxidation, the oxygen was absorbed by the oxygen carrier.

It can be observed that most of the CH_4 remained unconverted in the outlet. This was expected due to the low reactivity of ilmenite with methane at the chosen temperature level. Some CO and H_2 were formed at the end of the fuel pulse, and at the same time, the CO_2 concentration decreased. This was also expected since the oxidation state of the oxygen carrier is assumed to affect the total conversion and the form of the products.

Effect of K_2CO_3 addition on fluidization

The fluidization of the bed was evaluated qualitatively during the experiment by monitoring the pressure drop over the bed. The graphs in Fig. 5 show the pressure drop signal recorded during the four experiments. The experiments with salt addition are presented in the lower panel. In the two experiments without salt addition, the pressure drop behavior was constant throughout the whole experiment. Essentially, the signal fluctuated with a similar frequency and amplitude. The center of the pressure drop curve was also constant, suggesting that the same amount of bed material was fluidized during the whole measurement. The same could be said about the K_2CO_3-addition experiment at 850°C (lower left graph, where the timing of the salt addition is included).

Greenhouse. Gas. Sci. Technol. **0**:1–20 (2023); DOI: 10.1002/ghg.2218

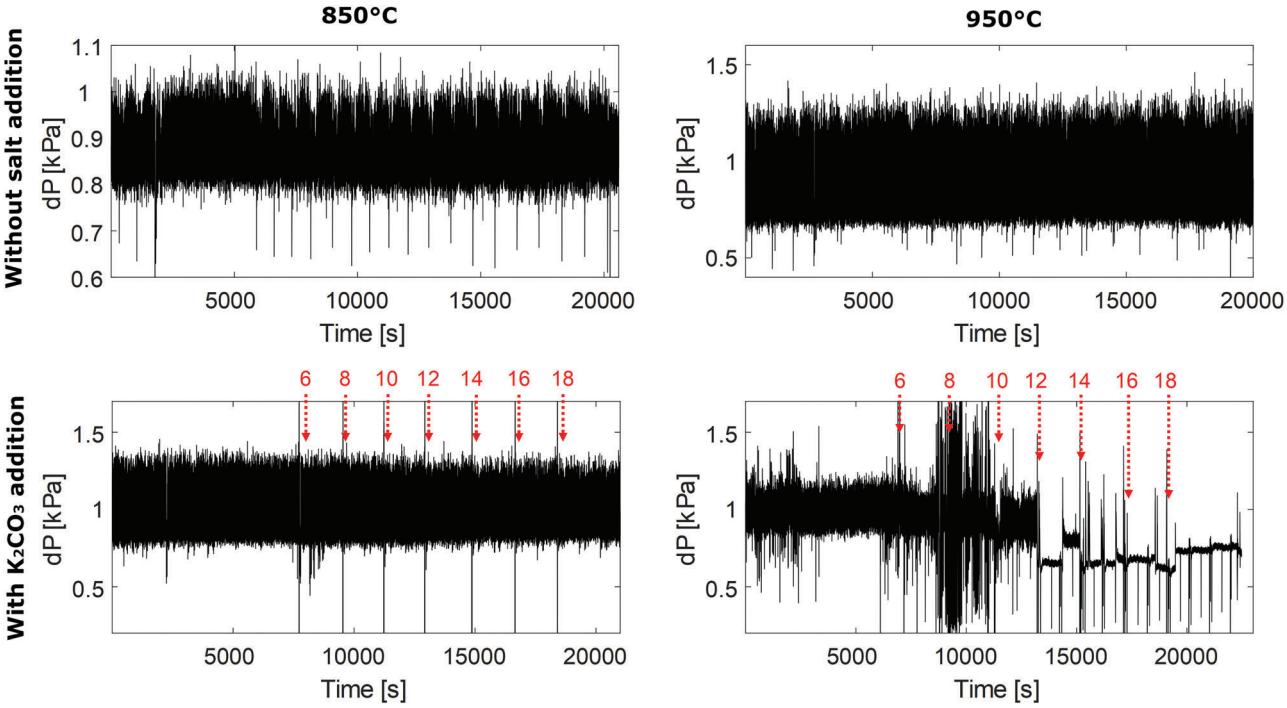

Figure 5. Pressure drop signals during the experiments. Upper row: experiments without salt addition, lower row: experiments with salt addition where the addition of K_2CO_3 and corresponding cycle numbers are indicated.

For the experiment with K_2CO_3 addition at 950°C, the pressure drop behavior changed throughout the experiment. There was an increase in amplitude after cycle 7, which is between the two first additions of K_2CO_3. A sudden decrease in both pressure drop and amplitude was then seen after about 2/3 of the experiment (at cycle 12), and this can be interpreted as defluidization. In total 900 mg of K_2CO_3 had then been added to the bed. This corresponds to 4.5% of the ilmenite weight in the reactor. This is in line with an experiment conducted by Zevenhoven et al., who saw defluidization after the addition of K_2CO_3 of what corresponded to 7.2% of the ilmenite weight,[22] although at a different pace. Also, that study was conducted under oxidizing conditions. It is expected that redox reactions, such as here, would contribute to different reaction mechanisms and more drastic changes in the material due to the continuous changes between reducing and oxidizing conditions.

A detailed view of the pressure drop in the 950°C experiment with K_2CO_3 addition is presented in Fig. 6. The figure shows the gas concentrations and the pressure measurements for cycles 11 and 12. The timing of the salt addition for the 12th cycle is marked in the figure. In the 11th reduction and oxidation phases, the bed was fluidized. The salt was then added which can be seen as a peak in the CO_2 concentration, starting at around 1,500 s. The CO_2 was released as the salt decomposed, which was seen at both 950 and 850°C. The pressure measurement showed that the defluidization coincided with the addition (and decomposition) of the salt. In the 12th reduction phase, the bed was fluidized again for a short while before it was again defluidized. It then remained essentially the same for the rest of the experiment (the pressure drop during the whole experiment is seen in the lower right graph in Fig. 5).

Agglomeration was also investigated by visual examination of the sample after the experiment had been concluded. For all examined samples, the majority of the material was in the form of free particles, similar to the fresh material. For material operated at 850°C with K_2CO_3 addition, separate white grains were found in the sample, in addition to a few, small dark lumps of bed material. Elemental analysis (SEM-EDS) of the white grains showed that it was a K- and O-rich phase, resulting from the added K_2CO_3. Thermodynamic data for K_2CO_3 states that it is quite stable in the presence of CO_2 and the melting point of K_2CO_3 is around 900°C (the melting and evaporation

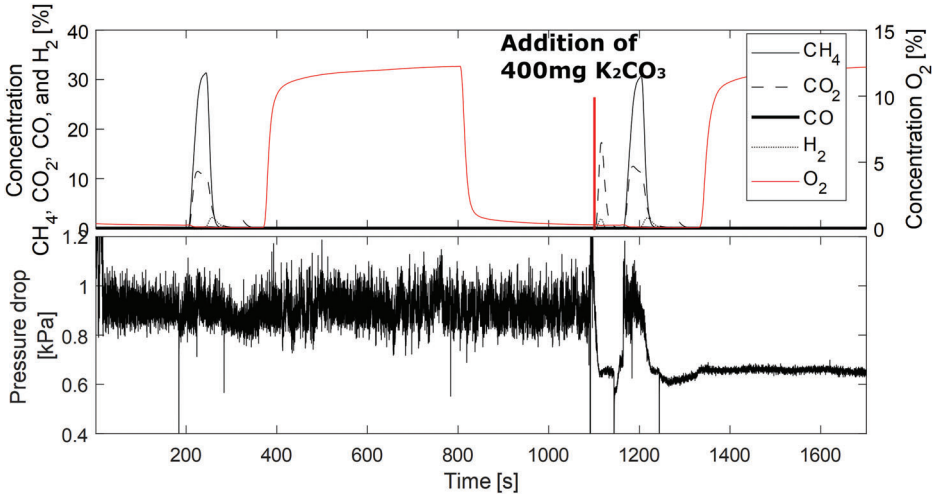

Figure 6. Concentrations and pressure drop for cycles 11 and 12, showing that defluidization coincides with the addition of K_2CO_3 to the bed. The addition of 400 mg of K_2CO_3 is indicated.

of decomposition products are more complex[43]). It was therefore not surprising to see salt crystals remaining as separate particles in the bed at 850°C. In the sample from K_2CO_3-addition at 950°C, lumps of ilmenite had formed which explained why the fluidization was negatively affected. Most of the lumps were in the form of hard spheres with a diameter of a few millimeters. A few larger agglomerates were up to 1 cm long and irregular in shape. No white grains were found in the 950°C experiment with K_2CO_3-addition, most likely because all the salt melted and interacted with the ilmenite and/or evaporated from the bed.

Material analysis

The material analysis was done to determine if, and how, K interacted with the ilmenite in the K_2CO_3-addition experiments. The SEM/EDS analysis was done on many particles to get representative results. Analysis of the surface of particles from the experiments at 950°C showed 1.5-4 at.% of K and Fe/Ti ratio of about 1.5–3. Very similar results were obtained for the experiment at 850°C. The initial concentration of K in ilmenite is very low (less than 0.07 wt.-%[42]). Thus, the presence of K on the surface confirms that the particles have been in contact with the K added to the bed and that the method for salt addition has been successful.

The XRD analysis revealed that without K_2CO_3 present, the used material was in the form of pseudobrookite (Fe_2TiO_5), hematite, and magnetite which are the expected phases to form at a slightly reduced state. The sample from the 950°C experiment had a higher magnetite/hematite ratio than the 850°C experiment which is expected since the reduction was deeper at the higher temperature. Apart from that, the XRD results were similar at the two different temperatures. The addition of K_2CO_3 resulted in K-titanate phases forming at both 850 and 950°C. The suggested K-titanate phase was KTi_8O_{16}, but other, similar phases could not be excluded. The 950°C sample had a higher K-titanate/pseudobrookite ratio compared to the 850°C sample. This suggests that pseudobrookite to a larger extent remained intact at 850°C, but that Fe and Ti separated more into different phases at the higher temperature.

Cross-section SEM/EDS analysis of particles from the 850°C experiment with K_2CO_3-addition showed that no or very little K had diffused into the particles. The K-titanate found in XRD from this sample was therefore probably only present in a low concentration. On the other hand, the cross-section analysis for the experiment at 950°C and K_2CO_3-addition concluded that K had accumulated in the particles. Fe had accumulated on the particle surface and K was present underneath this layer, as can be seen in Fig. 7. The figure shows a micrograph of a particle (left) elemental distribution of Fe, K (middle), and Ti (right). The Fe and Ti in the particle were separated, and the K was seen in the Ti-rich locations. This is in line with the XRD analysis results and with previous studies that have found that K-titanates forms in ilmenite which at the same time enhances the separation of Fe and

Greenhouse. Gas. Sci. Technol. **0**:1–20 (2023); DOI: 10.1002/ghg.2218

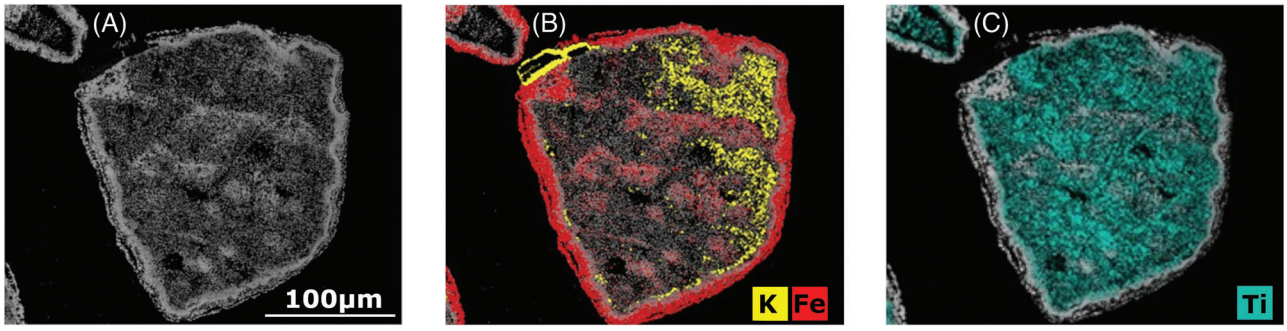

Figure 7. Elemental distribution obtained with SEM/EDS analysis. The sample is from the experiment at 950°C with addition of K_2CO_3. (a) Micrograph, (b) distribution of Fe in red, and K in yellow, (c) distribution of Ti in blue.

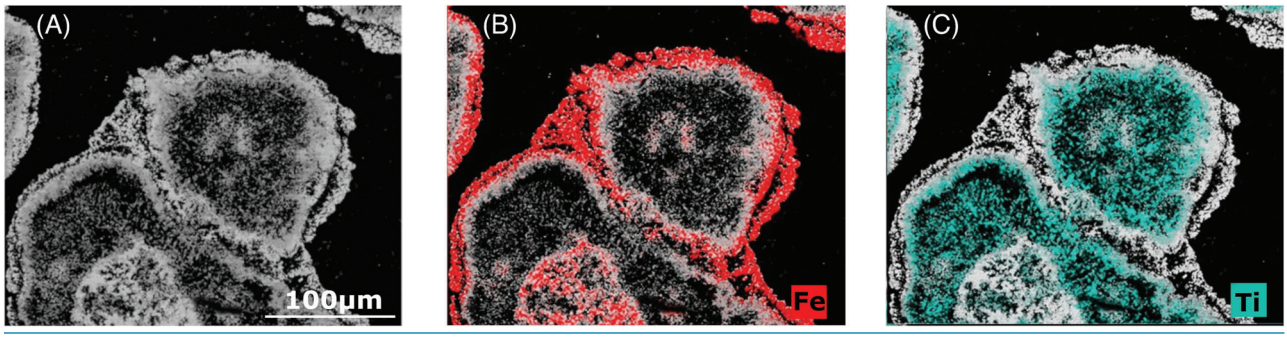

Figure 8. Elemental distribution obtained with SEM/EDS analysis. The sample is from the experiment at 950°C with addition of K_2CO_3. (a) Micrograph, (b) distribution of Fe in red, (c) distribution of Ti in blue.

Ti.[30,21] The mechanism has similarities with the industrial process known as alkali roasting.[45] Further, Fe has been seen to migrate to oxygen-rich surfaces by forming Fe_2O_3.[30,33]

The sample in the K_2CO_3-addition experiment at 950°C was clearly affected by the salt in terms of agglomeration. This was confirmed both by the pressure drop measurement and the visual inspection of the collected sample. Cross-section analysis was done on several sample particles to investigate the agglomeration mechanism. Contrary to what was first expected, no elevated K concentration was seen between the agglomerated particles. The Fe and Ti distributions of two agglomerated particles are presented in Fig. 8.

The analysis again showed a separation of Fe and Ti within the particle. The Fe had migrated and concentrated to the surface of the particles and an island in the bottom left of the figure. The analysis suggested that the sintering between the particles happened in a Fe-O-rich phase on the surface. There is no evidence that any eutectic point exists in the Fe-Ti-O phase diagram, thus, no melting is assumed to take place. Solid state sintering is therefore the suggested agglomeration mechanism. Solid-state sintering of ilmenite phases has been studied by Purnomo et al.[27] and was also suggested by Zevenhoven et al.[22] to take place in ilmenite mixed with K_2CO_3.

Based on these results, it can be concluded that the presence of K accelerated the migration of Fe to the surface and by that also increased the tendencies towards agglomeration. A few, very small lumps of material were also formed at 950°C without salt addition, and SEM/EDS analysis revealed a similar sintering mechanism. However, the sintering without salt addition happened to a much lower extent and fluidization was not affected.

Effect of K_2CO_3 addition on fuel conversion

The mass-based conversion of the oxygen carrier (presented as $100 - \omega_{\text{fInal}}$) versus cycle number is presented in Fig. 9. The figure shows the data obtained for the experiments without salt addition. Figure 9 also shows the yield of CO_2, CO, and CH_4 as defined previously. For comparison, with the parameters used in the experiment (20 g oxygen carrier and 40 s of

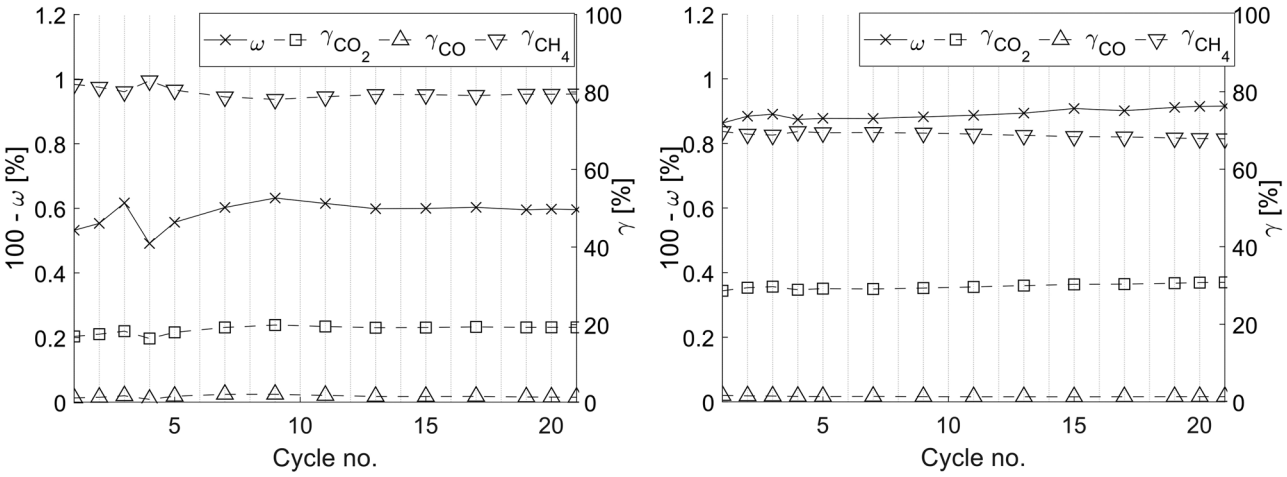

Figure 9. Mass-based conversion (100-ω_{final}), CO_2-yield (γ_{CO_2}), CO-yield (γ_{CO}), and CH_4-yield (γ_{CH_4}) as a function of cycle number for the experiments without salt addition. Left: 850°C, right: 950°C

reduction with 400 NmL/min methane), a total conversion from methane to CO_2 and H_2O corresponds to 100 − ω_{flnal} equal to 3.6%.

The conversion was higher at a higher temperature, which was expected. The CO yield was more or less constant at 1% throughout both experiments. The conversion at 850°C showed some variation in the beginning but was then more or less stable throughout the rest of the experiment. The activation was done mainly the day before the experiment which can explain some of the variations observed at the beginning of the experiments.

The 950°C experiment showed a slight continuous increase in mass-based conversion and CO_2 yield with cycle number. This could mean that the material became more activated during the 950°C experiment. Previous observations with ilmenite have found that the activation of ilmenite takes many cycles. Azis et al.[9] saw relatively stable CH_4 conversion after 35 cycles. Adánez et al.[33] saw ongoing structural changes in ilmenite still after 100 cycles with H_2 and H_2O as reducing gas. It is thus not surprising that the activation performed before these experiments (28 cycles) was insufficient to completely stabilize the activity of the material. In fact, it is not obvious that such a point will ever be reached. However, the 850°C-experiment did not show the same trend. Possibly, structural changes in the ilmenite were enhanced at higher temperatures.

Figure 10 shows the conversion and yields as a function of cycle number for the experiments with K_2CO_3-addition. The lower part of the figures shows the amount of salt added (accumulated).

When K_2CO_3 was added to the hot bed, it rapidly decomposed and CO_2 was released. This resulted in an initial CO_2 peak in the concentration data (visible in Fig. 6) which overlapped with the CO_2 from the fuel conversion. For this reason and to facilitate understanding, the cycles with salt feeding (cycles no. 6, 8, 10, 12, 14, 16, and 18) have been omitted from the graphs. Nevertheless, these cycles showed CO_2 concentrations in line with the expectations.

At 850°C, the methane conversion was more or less stable throughout the whole experiment apart from a slight deviation after the first salt feeding (cycle 6). At 950°C, the amount of unconverted methane increased after the first salt addition. Consequently, the mass-based conversion of the oxygen carrier and the CO_2 yield decreased. The conversion of methane to CO_2 then increased steadily throughout the whole experiment, without ever reaching the initial fuel conversion. A summary of the results is presented in Table 7.

There are a few ways in which an alkali ash component could affect the fuel conversion in CLC. Previous studies have shown examples of ash components forming impenetrable layers on the surface of the particles, creating a barrier between the oxygen carrier and the fuel. The ash layer could also cause agglomeration. Both layer formation and agglomeration would affect the conversion by decreasing the contact between the oxygen carrier and the fuel. This has been observed when KH_2PO_4 was added to a fixed bed of ilmenite[21] and a fixed bed of an iron oxygen carrier.[24] Another option found in the

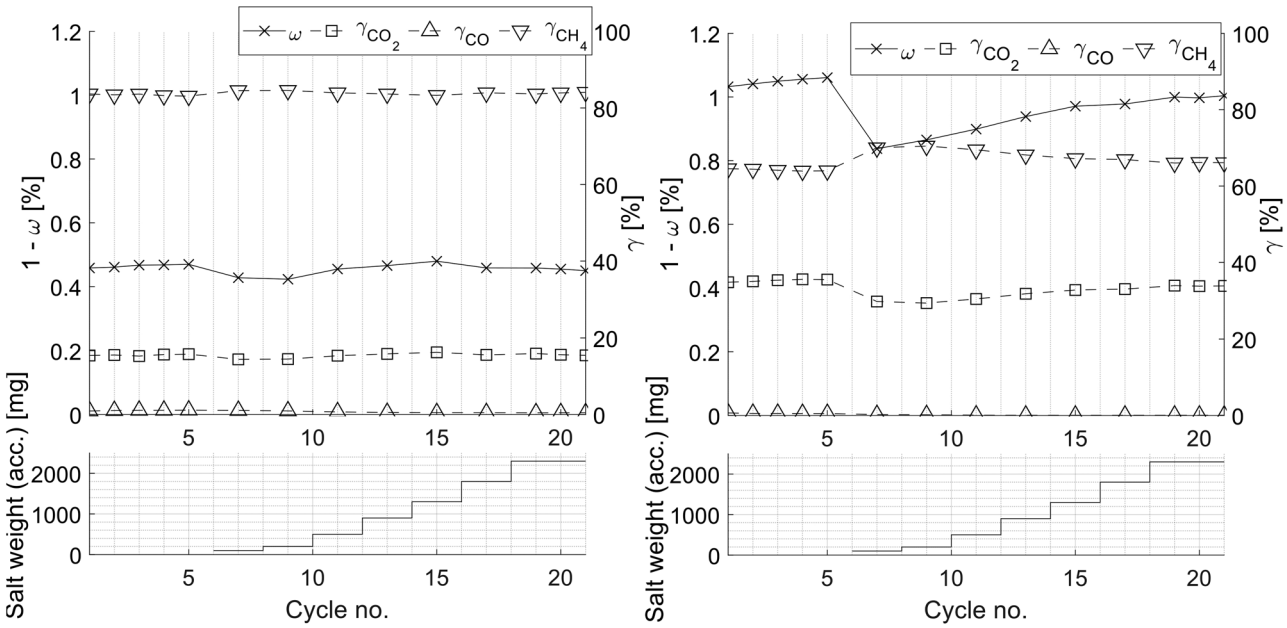

Figure 10. Mass-based conversion (100-ω_{final}), CO_2-yield (γ_{CO_2}), CO-yield (γ_{CO}), and CH_4-yield (γ_{CH_4}), as a function of cycle number for the experiments with K_2CO_3-addition. Left: 850°C, right: 950°C. The lower panels show the accumulated addition of K_2CO_3 (in mg; see Table 6).

Table 7. Summary of the experimental findings.

Salt	T(°C)	Fuel conv.	Pressure drop	Sample appearance	Material analysis
-	850°C	Stable	Uniform	Mainly free particles.	
-	950°C	Small increase	Uniform	Few small clumps of agglomerates. Mainly free particles.	Agglomerates have bridges/necks with Fe.
K_2CO_3	850°C	Stable	Uniform	Few small clumps of agglomerates (a few mm). Mainly free particles. White grains of salt.	Even dist. of K on the surface. No/very little K in the interior of particles. Presence of K-titanate.
K_2CO_3	950°C	Sharp decrease, slow increase	Sudden decrease in level and amplitude	Many small round clumps of agglomerates. Some large lumps, but mainly free particles.	Even dist. of K on the surface. K is present in the interior of particles. Presence of K-titanate. Agglomerates have bridges/necks with Fe.

literature is that the presence of K actually increases fuel conversion with ilmenite. Bao et al.[46] found that ilmenite doped with K had a higher fuel reactivity than ilmenite without. They suggested that the increased reactivity was because the diffusion of K into the particle promoted pore formation in the material structure. They showed that the BET surface area (and consequently fuel-oxygen carrier contact) of K-doped ilmenite increased with K-concentration. The same trend was seen by Hildor et al.,[21] who found from fixed bed interactions between ilmenite and K_2CO_3 that the reduction of ilmenite was faster when K_2CO_3 was present. They suggested, however, that the increased reduction rate was due to the enhanced iron migration taking place when K separates ilmenite into K-titanate and iron oxide.

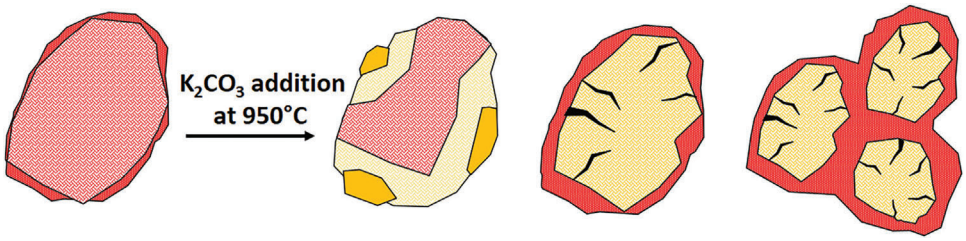

Figure 11. A suggested development of ilmenite during the 950°C with K_2CO_3 addition, starting with an activated ilmenite particle (left). K in yellow, Fe in red.

In the present case, the initial drop in fuel conversion at 950°C could possibly be due to the formation of agglomerates, which would negatively affect the solid-gas contact in the bed. However, this is not supported by the pressure drop signal, showing no or very little effect on the fluidization after the first salt addition. A part of the explanation lay in how the particles develop over time. A suggested interaction path is illustrated in the lower part of Fig. 11. Assuming that the K-diffusion into the fresh ilmenite was initially slow, layers of molten alkali could potentially form on the surface, causing slight agglomeration and a decreased solid-gas contact and fuel conversion. With time, the K diffused into the core and formed K-titanates with enhanced Fe-migration as a result. K-diffusion into the core, K-titanate formation, and enhanced Fe-migration were all observed in the material analysis. A continuous increase of Fe on the surface is in line with the later increased fuel conversion since Fe is the active oxygen-carrying phase of the ilmenite.

The K interaction process has previously been seen to increase pore formation in the ilmenite structure,[46] meaning that salt added at a later stage in the experiment would have a path for quickly diffusing into the core of the ilmenite structure. Therefore, no melt formation on the surface was found in the SEM/EDS analysis. When the particles finally sintered and defluidized due to Fe-phases on the particle surfaces, much of the active Fe-rich phase was still available for interactions with the gaseous fuel, as illustrated in the last stage of development in Fig. 11. Without salt present, the material looked more or less the same as before the experiment, with some Fe enrichment on the surface originating mainly from the calcination and activation of the ilmenite.

An alternative explanation for the decrease in fuel conversion observed with salt addition could be that gas phase alkali is known to inhibit full conversion of fuel in conventional combustion.[47,14] However, assuming that CO is an intermediate reaction product in methane conversion, this should result in elevated CO emissions which have not been observed. At both temperatures, the CO yield was low after salt addition and the conversion of CH_4 resulted in almost only CO_2. Further, the fuel conversion in the current process is not through gas-gas interactions. The presence of gas-phase K is thus assumed not to be the explanation for the decreased fuel conversion.

Discussion about the new method

One of the goals of this study was to develop an improved lab-scale method for the controlled addition of an ash model compound to a hot fluidized bed reactor capable of simulating CLC conditions. Here, the addition of alkali salt as a model compound is a crucial step. The alkali should be inserted close to the bed material and have enough residence time to have the possibility to interact. It was confirmed with material analysis that K was present in the bed and on the surface of the particles. Thus, it was concluded that the proposed method for ash interaction studies was successful for the current ash model compound (K_2CO_3). Further, no problems such as clogging of the feeding pipe or downstream filters of the reactor were detected during the experiments. It was also established that no significant amounts of salt were stuck on the reactor walls.

The mechanical conditions inside the reactor are different from that of industrial systems with higher gas velocities.[41] The setup is therefore not suitable for drawing conclusions on attrition etc. Nevertheless, the advantage of operating at this scale is that parameters are easily altered and it is possible to test extreme conditions, such as those found in hot spots or oxygen-depleted zones. Good mixing and homogeneity

throughout the bed can be assumed. Finally, mass and elemental balances can more easily be solved on this scale, and when using a batch reactor setup.

Conclusions

Interactions between ilmenite and K_2CO_3 were studied in a lab-scale fluidized bed reactor simulating CLC conditions. The performance of ilmenite at an increasing load of K_2CO_3 was studied with respect to fluidization and fuel conversion. A new reactor and an improved experimental method were developed and evaluated for this study, and the results are relevant for the conversion of biomass with solid oxygen carriers. Biomass ash interactions with ilmenite under different conditions have been studied previously, but the current system and method provide improved possibilities to isolate the Fe-Ti-K system and study it separated from other ash compounds under fluidizing and reducing conditions. Material analysis was conducted to evaluate the chemical and morphological changes of the material.

The following conclusions were drawn from the study:

- The addition of K_2CO_3 to ilmenite during CLC simulation increased the tendency for agglomeration at 950°C. The defluidization was sudden and happened during the inert phase immediately after the addition of the salt. The suggested mechanism was solid sintering between the iron oxides on the surfaces of the particles.
- The addition of K_2CO_3 to ilmenite during CLC simulation at 950°C had some negative effects on the CH_4 conversion. However, the decrease in fuel conversion was temporary and did not increase with an increased amount of K_2CO_3 added to the bed.
- Interaction between ilmenite and K_2CO_3 was observed to take place at 850°C resulting in the formation of K-titanates, but the limited interaction did not affect the fluidization or the fuel conversion.
- The new reactor and method were suitable for studying the interactions between K_2CO_3 and bed material in a hot fluidized lab-scale unit. This conclusion was based on the material analysis of samples from K-addition experiments that showed the presence of K in the core and on the surface of the particles. It is therefore of interest to extend the experiments to include more ash model compounds and other oxygen carriers in this setup.

Acknowledgments

This research was funded by the Swedish Research Council, project number 2017–04553 Combustion of biomass by Oxygen Carrier Aided Combustion. This work was performed in part at the Chalmers Material Analysis Laboratory, CMAL. Rustan Hvitt is acknowledged for the construction of the reactor. Victor Purnomo is acknowledged for helping with the XRD analysis.

References

1. Coppola A, Scala F. Chemical looping for combustion of solid biomass: a review. Energy and Fuels. 2021;35(23):19248–65.
2. Adánez J, Abad A, Mendiara T, Gayán P, de Diego LF, García-Labiano F. Chemical looping combustion of solid fuels. Prog Energy Combust Sci. 2018;65:6–66.
3. Thunman H, Lind F, Breitholtz C, Berguerand N, Seemann M. Using an oxygen-carrier as bed material for combustion of biomass in a 12-MWth circulating fluidized-bed boiler. Fuel. 2013;113(x):300–9.
4. Stenberg V, Rydén M, Mattisson T, Lyngfelt A. Experimental investigation of oxygen carrier aided combustion (OCAC) with methane and PSA off-gas. Appl Sci. 2021;11(1):1–25.
5. Störner F, Lind F, Rydén M. Oxygen carrier aided combustion in fluidized bed boilers in Sweden — review and future outlook with respect to affordable bed materials. Appl Sci. 2021;11(17):7935.
6. Lind F, Corcoran A, Andersson B-Å, Thunman H. 12,000 hours of operation with oxygen-carriers in industrially relevant scale. VGB PowerTach. 2017;7:1–6.
7. Moldenhauer P, Corcoran A, Thunman H, Lind F. A scale-up project for operating a 115 MWth biomass-fired CFB boiler with oxygen carriers as bed material. In 5th international conference on chemical-looping, September 24—27, Park city, UT; 2018. Available from: https://research.chalmers.se/publication/505154/file/505154_Fulltext.pdf
8. Akademi Å. Åbo akademi university chemical fractionation database. [Internet] [cited: 29-Jun-2022]. Available from: https://web.abo.fi/fak/tkf/ook/bransle/database.php.
9. Azis MM, Leion H, Jerndal E, Steenari BM, Mattisson T, Lyngfelt A. The effect of bituminous and lignite ash on the performance of ilmenite as oxygen carrier in chemical-looping combustion. Chem Eng Technol. 2013;36(9):1460–8.
10. Grimm A, Skoglund N, Boström D, Öhman M. Bed agglomeration characteristics in fluidized quartz bed combustion of phosphorus-rich biomass fuels. Energy and Fuels. 2011;25(3):937–47.
11. Khan AA, de Jong W, Jansens PJ, Spliethoff H. Biomass combustion in fluidized bed boilers: potential problems and remedies. Fuel Process Technol. 2009;90(1):21–50.
12. Nunes LJR, Matias JCO, Catalão JPS. Biomass combustion systems: a review on the physical and chemical properties of the ashes. Renew Sustain Energy Rev. 2016;53:235–42.
13. Zevenhoven M, Yrjas P, Hupa M. Handbook of combustion, chapter 14: Ash-forming matter and ash-related problems. (Vol. 4). Weinheim, Germany: Wiley-VCH; 2010.
14. Berdugo Vilches T, Weng W, Glarborg P, Li Z, Thunman H, Seemann M. Shedding light on the governing mechanisms for

insufficient CO and H2 burnout in the presence of potassium, chlorine and sulfur. Fuel. 2020;273(January):117762.
15. Hindiyarti L, Frandsen F, Livbjerg H, Glarborg P. Influence of potassium chloride on moist CO oxidation under reducing conditions: Experimental and kinetic modeling study. Fuel. 2006;85(7–8):978–88.
16. Zevenhoven R, Kilpinen P. Chapter 8: Trace elements, alkali metals. In: Control of pollutants in flue gases and fuel gases. Helsinki University of Technology; 2001.
17. Piotrowska P, Zevenhoven M, Davidsson K, Hupa M, Åmand L-E, Barišić V, et al. Fate of alkali metals and phosphorus of rapeseed cake in circulating fluidized bed boiler part 1: cocombustion with wood. Energy and Fuels. 2010;24(1):333–45.
18. Leffler T, Brackmann C, Berg M, Aldén M, Li Z. Online alkali measurement during oxy-fuel combustion. Energy Procedia. 2017;120:365–72.
19. Mason PE, Jones JM, Darvell LI, Williams A. Gas phase potassium release from a single particle of biomass during high temperature combustion. Proc Combust Inst. 2017;36(2):2207–15.
20. Andersson V, Ge Y, Kong X, Pettersson JBC. A novel method for on-line characterization of alkali release and thermal stability of materials used in thermochemical conversion processes. Energies. 2022;15(12):4365.
21. Hildor F, Zevenhoven M, Brink A, Hupa L, Leion H. Understanding the interaction of potassium salts with an ilmenite oxygen carrier under dry and wet conditions. ACS Omega. 2020;5(36):22966–77.
22. Zevenhoven M, Sevonius C, Salminen P, Lindberg D, Brink A, Yrjas P, et al. Defluidization of the oxygen carrier ilmenite – laboratory experiments with potassium salts. Energy. 2018;148:930–40.
23. Staničić I, Hanning M, Deniz R, Mattisson T, Backman R, Leion H. Interaction of oxygen carriers with common biomass ash components. Fuel Processing Technology. 2020;200:106313.
24. Störner F, Hildor F, Leion H, Zevenhoven M, Hupa L, Rydén M. Potassium ash interactions with oxygen carriers steel converter slag and iron mill scale in chemical-looping combustion of biomass - experimental evaluation using model compounds. Energy and Fuels. 2020;34(2):2304–14.
25. Kuba M, Skoglund N, Öhman M, Hofbauer H. A review on bed material particle layer formation and its positive influence on the performance of thermo-chemical biomass conversion in fluidized beds. Fuel. 2020;291:120214.
26. Sevonius C, Yrjas P, Hupa M. Defluidization of a quartz bed - Laboratory experiments with potassium salts. Fuel. 2014;127:161–8.
27. Purnomo V, Yilmaz D, Leion H, Mattisson T. Study of defluidization of iron- and manganese-based oxygen carriers under highly reducing conditions in a lab-scale fluidized-bed batch reactor. Fuel Process Technol. 2021;219:106874.
28. Leion H, Lyngfelt A, Johansson M, Jerndal E, Mattisson T. The use of ilmenite as an oxygen carrier in chemical-looping combustion. Chem Eng Res Des. 2008;86(9):1017–26.
29. Leion H, Mattisson T, Lyngfelt A. Solid fuels in chemical-looping combustion. Int J Greenh Gas Control. 2008;2(2):180–93.
30. Corcoran A, Knutsson P, Lind F, Thunman H. Mechanism for migration and layer growth of biomass ash on ilmenite used for oxygen carrier aided combustion. Energy and Fuels. 2018;32(8):8845–56.
31. Corcoran A, Marinkovic J, Lind F, Thunman H, Knutsson P, Seemann M. Ash properties of ilmenite used as bed material for combustion of biomass in a circulating fluidized bed boiler. Energy and Fuels. 2014;28(12):7672–9.
32. Gyllén A, Knutsson P, Lind F, Thunman H. Magnetic separation of ilmenite used as oxygen carrier during combustion of biomass and the effect of ash layer buildup on its activity and mechanical strength. Fuel. 2020;269:117470.
33. Adánez J, Cuadrat A, Abad A, Gayán P, Diego LFD, García-Labiano F. Ilmenite activation during consecutive redox cycles in chemical-looping combustion. Energy and Fuels. 2010;24(2):1402–13.
34. Staničić I, Brorsson J, Hellman A, Mattisson T, Backman R. Thermodynamic analysis on the fate of ash elements in chemical looping combustion of solid fuels—iron-based oxygen carriers. Energy and Fuels. 2022;36(17):9648–59.
35. Eriksson JE, Zevenhoven M, Yrjas P, Brink A, Hupa L. Corrosion of heat transfer materials by potassium-contaminated ilmenite bed particles in chemical-looping combustion of biomass. Energies. 2022;15(8):2740.
36. Gogolev I, Soleimanisalim AH, Linderholm C, Lyngfelt A. Commissioning, performance benchmarking, and investigation of alkali emissions in a 10 kWth solid fuel chemical looping combustion pilot. Fuel. 2021;287: 119530.
37. Staničić I, Andersson V, Hanning M, Mattisson T, Backman R, Leion H. Combined manganese oxides as oxygen carriers for biomass combustion — ash interactions. Chem Eng Res Des. 2019;149:104–20.
38. Yilmaz D and Leion H. Interaction of iron oxygen carriers and alkaline salts present in biomass-derived ash. Energy and Fuels. 2020;34(9):11143–53.
39. Mei D, Lyngfelt A, Leion H, Mattisson T. Study of the interaction between a Mn ore and alkali chlorides in chemical looping combustion. Fuel. 2023;344:128090.
40. Andersson V, Soleimanisalim AH, Kong X, Hildor F, Leion H, Mattisson T. Alkali-wall interactions in a laboratory-scale reactor for chemical looping combustion studies. Fuel Process Technol. 2021;217:106828.
41. Leion H, Frick V, Hildor F. Experimental method and setup for laboratory fluidized bed reactor testing. Energies. 2018;11(10):2505.
42. Leion H, Mattisson T, Lyngfelt A. Use of ores and industrial products as oxygen carriers in chemical-looping combustion. Energy and Fuels. 23:2307–15, 2009.
43. Lehman RL, Gentry JS, Glumac NG. Thermal stability of potassium carbonate near its melting point. Thermochim Acta. 1998;316:1–9.
44. Boström D, Skoglund N, Grimm A, Boman C, Öhman M, Broström M. Ash transformation chemistry during combustion of biomass. Energy and Fuels. 2012;26(1):85–93.
45. El-Tawil SZ, Morsi IM, Yehia A, Francis AA. Alkali reductive roasting of ilmenite ore. Can Metall Q. 1996;35(1):31–37.

46. Bao J, Li Z, Cai N. Promoting the reduction reactivity of ilmenite by introducing foreign ions in chemical looping combustion. Ind Eng Chem Res. 2013;52(18):6119–28.

47. Rydén M, Hanning M, Lind F. Oxygen carrier aided combustion (OCAC) of wood chips in a 12 MW th circulating fluidized bed boiler using steel converter slag as bed material. Appl Sci. 2018;8(12):2657.

Felicia Störner

Felicia Störner is a PhD student at Chalmers. Her research is on utilizing low-cost materials and by-products from metallurgical industries as oxygen carriers in chemical-looping combustion and oxygen carrier aided combustion (OCAC). Her work focuses on studying interactions between oxygen carriers and biomass ash.

Pavleta Knutsson

Pavleta Knutsson is an associate professor, her work focuses on screening different types of oxygen carriers to use for chemical-looping combustion and gasification. Her focus is on surface chemistry, catalytic activity, and ash interactions of oxygen carriers. She is an expert in material characterization.

Henrik Leion

Henrik Leion is an associate professor, his research focuses on developing new low cost oxygen carriers and investigating the reactions between fuel and oxygen carriers in chemical-looping combustion and gasification. He has a long experience in evaluating oxygen carriers in small scale batch CLC simulations.

Tobias Mattisson

Tobias Mattisson is a professor, he is a leading researcher in the topic of chemical-lopping combustion and oxygen carriers and has over 20 years of experience in the field. His work includes, among other topics, screening of oxygen carriers, thermodynamic evaluations, chemical-looping combustion of solid fuels and alkali interactions.

Magnus Rydén

Magnus Rydén The main research area of associate professor Magnus Rydén is chemical-looping combustion, conversion of fuels into gaseous hydrogen and combustion and gasification of biomass in fluidized beds. His work ranges from lab-scale up to industrial scale oxygen carrier aided combustion, including testing different oxygen carriers in industrial oxygen carrier aided combustion settings.